Radboud Repository

Radboud University Nijmegen

PDF hosted at the Radboud Repository of the Radboud University Nijmegen

The following full text is a publisher's version.

For additional information about this publication click this link.
http://hdl.handle.net/2066/21309

Please be advised that this information was generated on 2017-12-05 and may be subject to change.

ELSEVIER

Brain Research 689 (1995) 47–60

BRAIN RESEARCH

Research report

The hypothalamic paraventricular nucleus in two types of Wistar rats with different stress responses. I. Morphometric comparison

W.H.A.M. Mulders [a,*], J. Meek [a], T.G.M. Hafmans [a], A.R. Cools [b]

[a] *Department of Anatomy and Embryology, University of Nijmegen, Geert Grooteplein Noord 21, PO Box 9101, 6500 HB Nijmegen, The Netherlands*
[b] *Department of Psychoneuropharmacology, University of Nijmegen, Geert Grooteplein Noord 21, PO Box 9101, 6500 HB Nijmegen, The Netherlands*

Accepted 18 April 1995

Abstract

The present study evaluates the role of the hypothalamic paraventricular nucleus (PVH) in stress regulation by a morphometric comparison of the vascular, neuronal and synaptic properties of this nucleus in two lines of Wistar rats. It has been previously reported that these two lines of rats, indicated as APO-SUS (apomorphine-susceptible) and APO-UNSUS (apomorphine-unsusceptible) rats on the basis of their reactivity to a subcutaneous injection of apomorphine, display a variety of pharmacological and behavioral differences, including differences in their stress-coping mechanisms (Cools et al., *Neuropsychobiology*, 28 (1993) 100–105). The results show a similar vascular and neuronal organization of the PVH in both lines, but distinct synaptic differences. The PVH (0.12 mm^3 volume with about 15,000 neurons on one side) has an overall vascular density of 5.6%, with significant differences between subdivisions (parvocellular central part: 8.3%, parvocellular dorsal/ventral/posterior part: 4.6–5.3%), which means that vascularity is a useful tool to delineate subdivisions in the parvocellular PVH. The neuronal density of $132 \times 10^3/mm^3$ as found in the present study is two times higher than reported in a previous study (Kiss et al., *J. Comp. Neurol.*, 313 (1991) 563–573). Possible reasons for this discrepancy are extensively discussed. The most significant finding of the present study is the observation that APO-SUS rats have a significantly higher synaptic density ($158 \times 10^6/mm^3$) in the PVH than APO-UNSUS rats ($108 \times 10^6/mm^3$). It is discussed in which way this synaptic difference may be correlated with the different activity of the hypothalamo-pituitary-adrenal axis in both lines of Wistar rats.

Keywords: Hypothalamic paraventricular nucleus; Morphometry; Stress; Synaptic organization; Vascularity; Wistar rat

1. Introduction

The hypothalamic paraventricular nucleus (PVH) plays an important role in the coordination of stress responses [10,35]. It contains a large number of corticotropin-releasing hormone (CRH) producing cells [6,44,46], which project to the neurohaemal zone of the median eminence [24,42,44,52], where CRH is released into the portal pituitary vessels. In the pituitary, CRH stimulates the secretion of ACTH, which in turn regulates the corticosteroid production in the adrenal cortex [32,46]. In this way the PVH stimulates the pituitary-adrenocortical activity in response to a variety of stressful situations [20,28,49].

A useful model to study the neuroanatomical basis of stress control is presented by two lines of Wistar rats with different stress responses [13–15,41]. These two lines have been pharmacogenetically selected on the basis of their gnawing responses after a subcutaneous injection of apomorphine, and are indicated as APO-SUS (apomorphine-susceptible) and APO-UNSUS (apomorphine-unsusceptible) rats, showing a high and a low gnawing response, respectively, after an identical dose of apomorphine [13]. Other differences can be observed in an open field test situation, in which APO-SUS rats show more locomotor activity, slower habituation and more edge-hugging behavior than APO-UNSUS rats. In the so-called defeat test, in which the rat is confronted with a much larger rat, APO-SUS rats show fleeing behavior, whereas APO-UNSUS rats exhibit freezing [13]. These interline differences are probably induced by different levels of circulating plasma-corticosteroids during the early postnatal period [13,15], which might well cause differences in the PVH of both lines. The fact that the ACTH-response to exogenous CRH-administration is more pronounced in APO-SUS than in APO-UNSUS rats [48], also suggests differences between the PVH of both lines. The aim of the present study is to investigate whether quantitative morphological pa-

* Corresponding author. Fax: (31) (80) 61-3789.

0006-8993/95/$09.50 © 1995 Elsevier Science B.V. All rights reserved
SSDI 0006-8993(95)00534-X

rameters in the PVH differ between APO-SUS and APO-UNSUS rats. Knowledge of such differences may contribute to a better understanding of the mechanisms giving rise to the line differences in responses to stress.

Previous morphometric studies of the PVH have been presented by Armstrong et al. [7], Swanson and Kuypers [42], Van den Pol [47], Swanson et al. [45] and Kiss et al. [23]. These authors have determined the numbers, sizes,

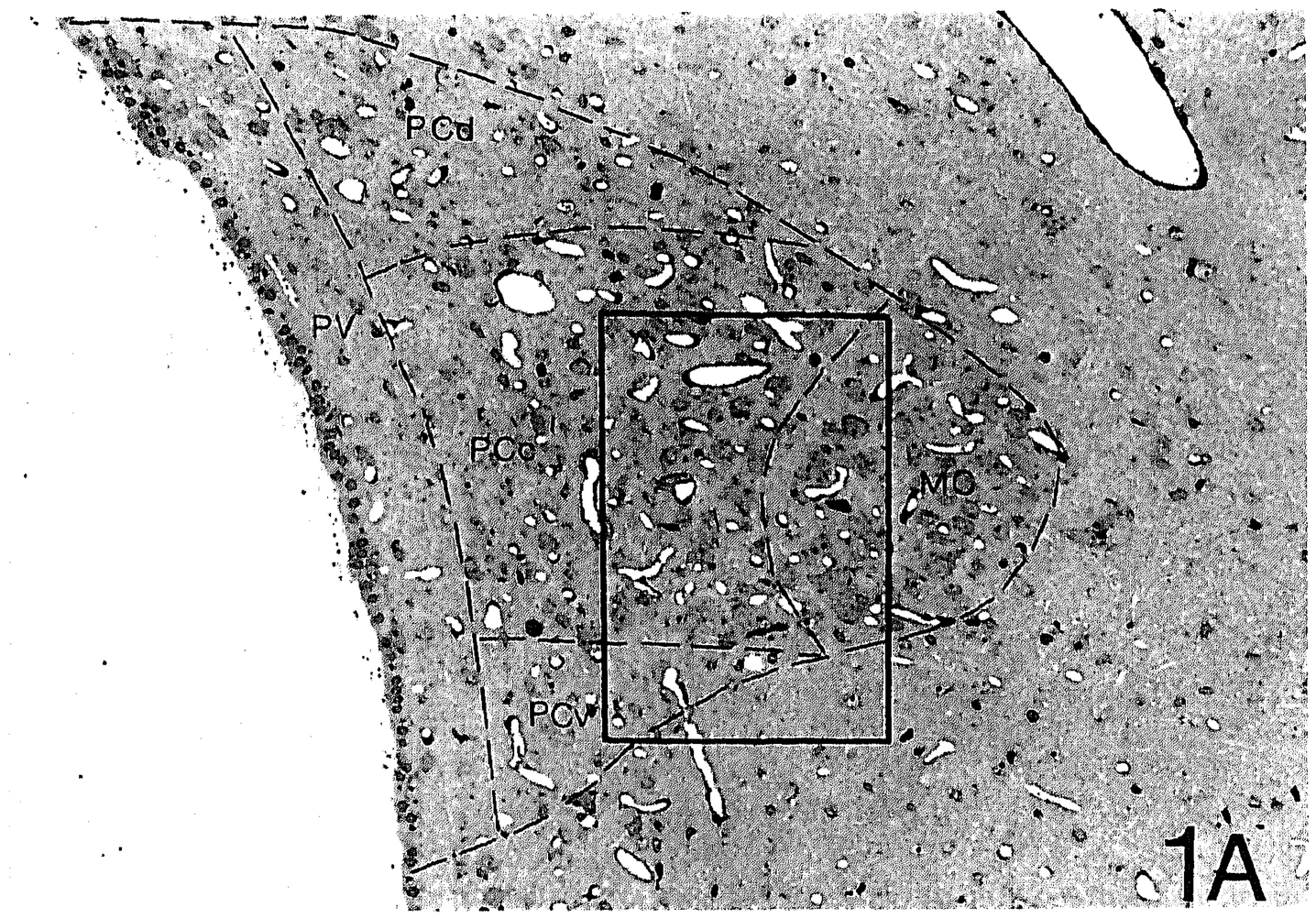

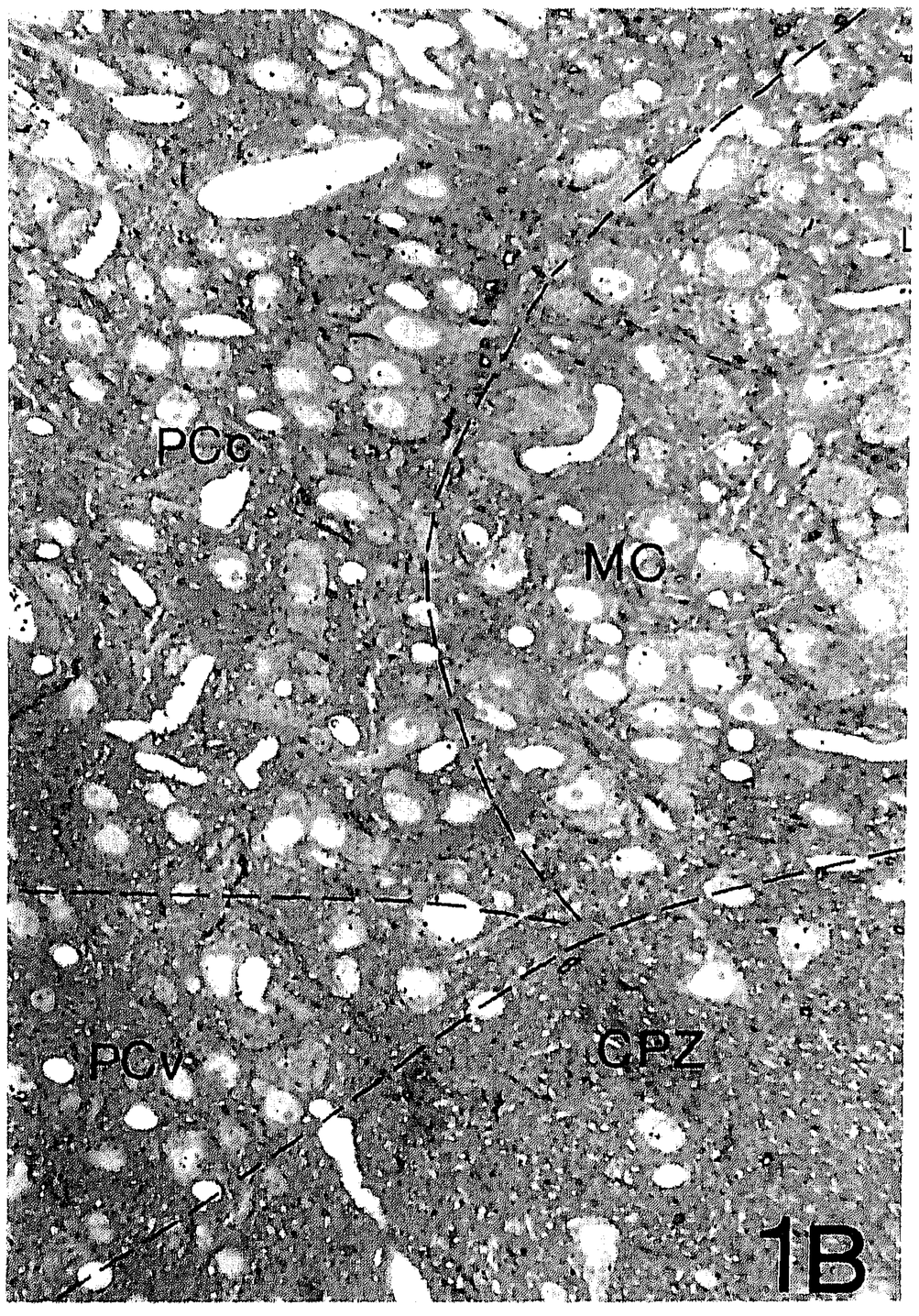

Fig. 1. A: photomicrograph of semithin (1 μm) section at the third level (see Fig. 2), stained with toluidine blue, at a magnification of 135 ×, showing different subdivisions. B: detailed photomicrograph of the indicated rectangular area in Fig. 1A, stained with paraphenylene-diamine, showing the somata with nuclei and nucleoli at a magnification of 340 ×. CPZ = cell poor zone; MC = magnocellular part; PCc = central parvocellular part; PCd = dorsal parvocellular part; PCv = ventral parvocellular part; PV = periventricular part.

shapes and densities of neurons in the different subdivisions of the PVH [7,23,42,45] or described the morphological and synaptic properties of PVH neurons qualitatively [47]. Quantitative data on the synaptic organization of the different subdivisions are lacking, however. The present study extends the previous morphometric data to the

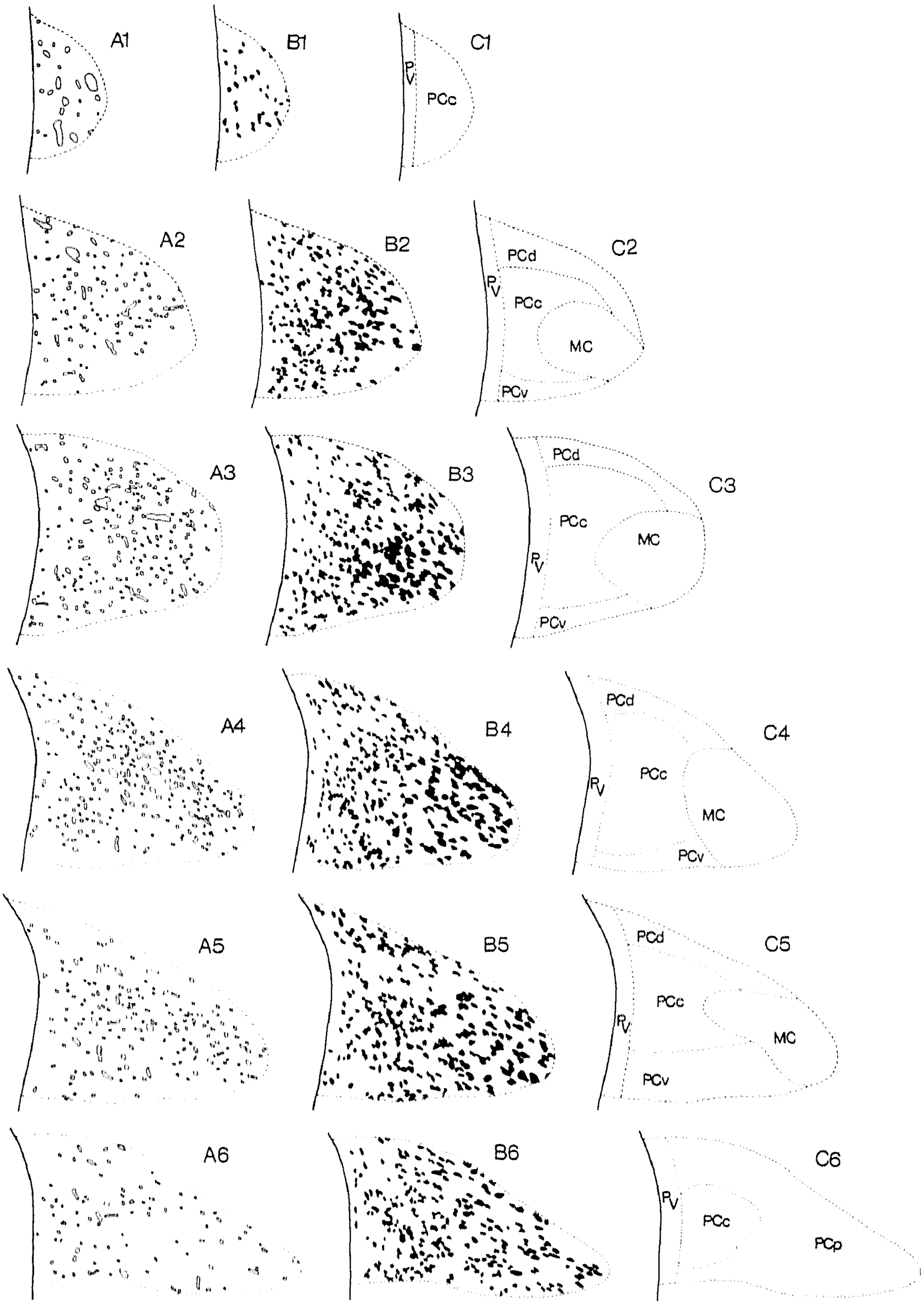

Fig. 2. Drawings of a representative series of six 1 μm thick Epon embedded sections of the left PVH with 75 μm intervals, stained with paraphenylene-diamine. At each level three separate drawings show the vascular profiles (A1...A6), neuronal profiles (B1...B6) and subdivisions (C1...C6). Magnification 44 ×. PCp = posterior parvocellular part. For other abbreviations see Fig. 1.

synaptic level, and contributes to an evaluation of the significance of some of the morphometric characteristics of the PVH by comparing functionally different rat strains.

2. Materials and methods

2.1. Animals

The quantitative morphometric data presented in this study are based on three male APO-SUS (F8 generation) and three male APO-UNSUS rats (F9 generation) of 200–250 g, bred in our Animal Laboratory. In addition, five normal Wistar rats were used to estimate the degree of tissue shrinkage involved in the present study. All rats were originally housed in groups of 2–3 animals per cage (36 × 24 × 25 cm) in a room with a constant temperature (20 ± 2°C) and a 06.00 to 18.00 h light period. Food and water were given ad libitum. Three days before the open field test APO-SUS and APO-UNSUS rats were isolated in single cages (36 × 24 × 25 cm) in the same conditions as mentioned above.

2.2. Tissue processing

After characterization in the open field test, the rats were deeply anesthetized with pentobarbital (6 mg/100 g b.wt.) and transcardially perfused with 100 ml saline (0.9% sodium chloride) followed by 450 ml of a 2% paraformaldehyde/2% glutardialdehyde mixture in a 0.1 M phosphate buffer (PB, PH 7.3). Immediately after perfusion, the dorsal part of the skull was removed and the rats were placed in a stereotactic device to make a precisely transverse incision. This allowed for sectioning of all brains in the same transverse plane.

After removal out of the skull, the brains were placed overnight in the perfusion fluid. Subsequently, sections of 100 or 75 μm were cut on a vibratome in PBS (0.1 M phosphate buffered saline, pH 7.3). After rinsing in the same buffer, the sections were osmicated for one hour in 1% osmium tetroxide dissolved in 0.1 M PB, rinsed in PB, dehydrated in a graded series of ethanol, embedded in Epon 812 via propylene oxide and mounted in Epon 812 between a slide and coverslip coated with dimethyldichlorosilane solution (2% in 1,1,1-trichloroethane). The latter allows for easy removal of slide and coverslip when necessary for further sectioning.

After polymerization for two days at 60°C, the sections containing the left PVH were remounted on Epon blocks for semithin and ultrathin sectioning. At intervals of 50 or 37.5 μm (in 100 μm and 75 μm vibratome sections, respectively), 1 μm thick semithin sections and adjacent 80 nm thick ultrathin sections were collected for morphometric analysis at the light and electron microscopic level, respectively. This procedure resulted in 10–12 PVH sample levels per animal. The semithin sections were stained with para-phenylene-diamine or toluidine blue and coverslipped with Entellan. The ultrathin sections were collected on 300 mesh copper grids and contrasted with uranylacetate and lead citrate.

2.3. Light microscopic analysis

For quantitative analysis of blood vessels and neurons, the semithin sections were studied and drawn using a Zeiss light microscope and drawing tube. First, the contour of the PVH was determined on the basis of the surrounding cell-sparse zone at a magnification of 130 × (Fig. 1A). Next, the PVH was subdivided on the basis of differentiations in neuronal size and density as well as vascular density (see Results and Fig. 1A,B and Fig. 2).

In each of the PVH subdivisions, blood vessels, nuclear profiles and somata containing a nucleus with a nucleolus were drawn at a magnification of 520 × at each sample level, using the paraphenylene diamine sections (Fig. 1B). The adjacent toluidine blue stained sections (Fig. 1A) were used to verify that exclusively neuronal profiles and no glial cells were drawn. The drawings obtained were used to determine the following parameters with the aid of a Kontron-Videoplan equipment: (1) the total surface area of the PVH and its different subdivisions, (2) the number, surface area and ellipticity of the nuclei sampled, and (3) the ellipticity and surface area of somata containing a nucleus with a visible nucleolus in the plane of sectioning. The latter was done to obtain a reliable neuronal diameter estimation [3,9,23,31]. From these data the volume of all PVH subdivisions and their average neuronal sizes, densities and numbers were calculated in a way that has been previously described by our group and others [1–3,17,36]. This method implies the following steps.

The volume of each PVH subdivision (V) was calculated by means of the Cavalieri principle [19,27,33,36], i.e. by multiplication of the mean surface area with the total length of each subdivision of the left PVH. At least 8 sample surfaces were measured for each subdivision, since this is a minimum for reliable estimations of V [26].

The mean neuronal diameter (D) was calculated from the surface area of somata containing a nucleus with a visible nucleolus in the plane of sectioning [3] as the D-circle. This is the diameter of a circle with the same surface area as the neuron traced.

Estimations of neuronal densities were based on nuclear tracings according to the formula presented by Floderus [17] and Abercrombie [2]:

$N_V = N_A/\overline{D} + t - 2h$ (see Royet (1991) for review [36]) in which:

N_V = number of neurons per unit volume,

N_A = number of nuclei per unit test area = N_{sample}/A_{sample},

$\overline{D}$ = the mean nuclear diameter,

t = the section thickness,

h = the height of the smallest recognizable cap.

To determine $\bar{D}$ and h the following formulae were used [40]:

$$\bar{D} = \bar{d} \cdot \left[1 - \left(\frac{(1 - 4/\pi)\bar{d}}{t + \bar{d}} \right) \right]$$

in which:
$\bar{d}$ = the mean profile diameter,
t = see above.
$h = R - \sqrt{(R_2 - r_o^2)}$ [51]
in which:
R = mean nucleus radius,
r_o = the radius of the smallest visible profile.

Neuronal numbers were calculated by multiplication of N_V and V per subdivision. The mean ellipticity index (smallest diameter divided by the largest diameter) of the nuclei was measured to be 0.62 ± 0.01, a value which allows for reliable estimations of neuronal densities with the formulae just explained [3,8].

Vascular densities were calculated by means of point counts [36,51]. A frame with points at 0.5 mm intervals was randomly positioned over the drawings made at a magnification of 520× and the points covering blood vessels as well as the total surface of each subdivision were counted. The volume fraction of blood vessels was calculated by dividing the number of points covering blood vessels by the number of points of the total area.

2.4. Electron microscopic analysis

For analysis of the ultrathin sections of the PVH, quantitative synaptic parameters were systematic randomly sampled in a Philips EM 301 electron microscope by taking photographs in every corner and center of each 300 mesh grid square at a magnification of about 19,000×. A replica of 2,160 lines/mm was used to measure the precise magnification. This procedure yielded on average 18 photographs per subdivision per PVH, with a minimum of 12

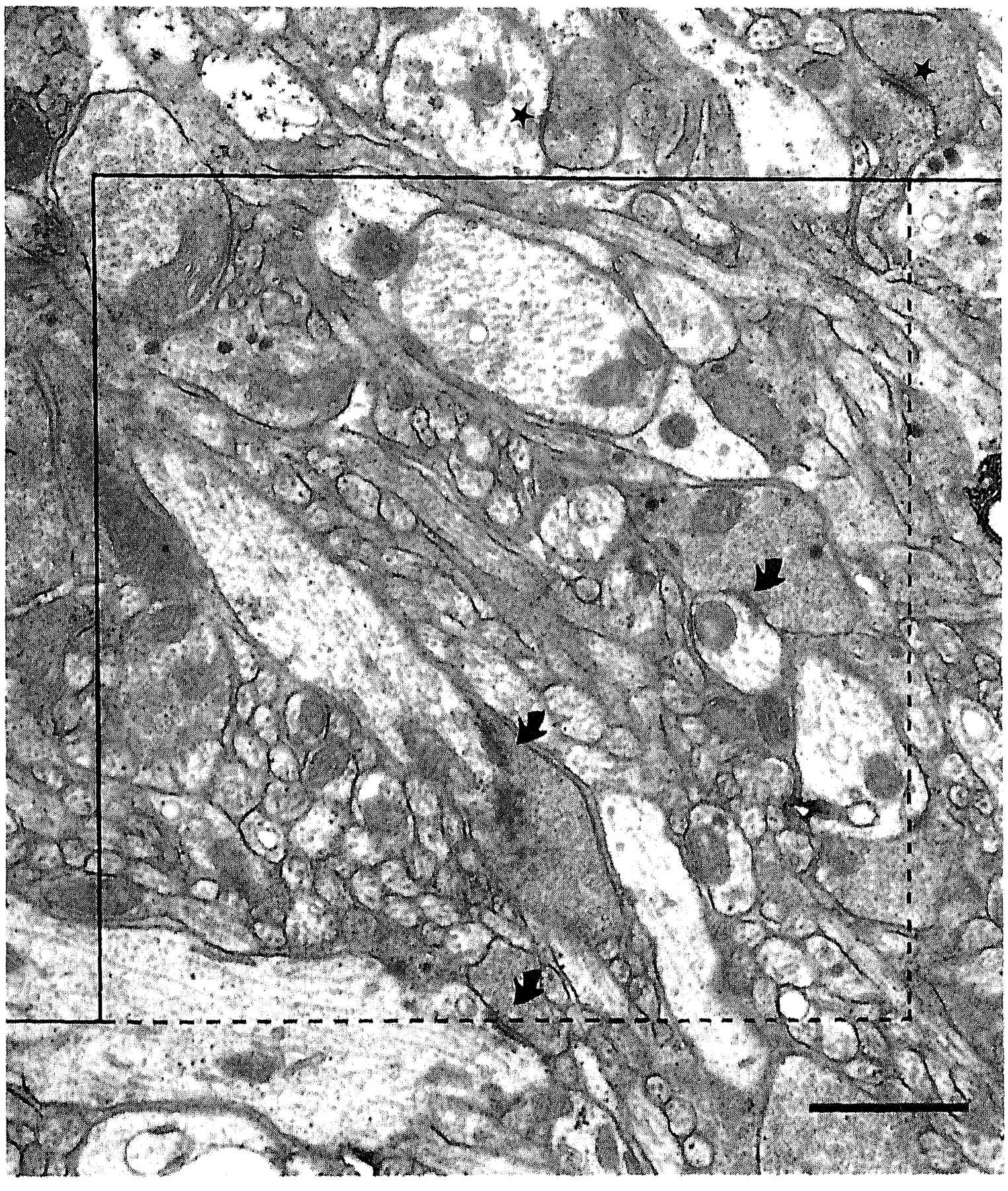

Fig. 3. Electron micrograph of a representative part of the PVH, showing synaptic contacts within (arrows) and outside (stars) the forbidden lines. Bar = 1 μm.

photographs for the PCd. On average each electron micrograph showed 2 synaptic contacts. It was verified that this procedure yielded stable average values and standard errors of the synaptic parameters determined. The location of the electron micrographs in the PVH was determined by comparison of low magnification electron micrographs of the sections analysed with the adjacent semithin sections used for LM analysis. Each electron micrograph was covered by a square test frame and all synaptic contacts within this test frame and not touching the forbidden lines [18,36] were traced on the Kontron-Videoplan equipment (Fig. 3).

From these measurements the mean synaptic contact trace length ($\bar{L}$) per subdivision was calculated and other parameters were determined as follows: The synaptic contact diameter was estimated on the basis of the formula: $\bar{D} = (4/\pi) \times \bar{L}$ [1,4,25]. The synaptic density (N_V) was determined with the formula: $N_V = N_A/\bar{L}$ [4,11,12], in which N_A is the number of profiles per area. The synapse to neuron (S/N) ratio was determined as the ratio of synaptic and neuronal density: N_V(synapse)/N_V(neuron).

2.5. Shrinkage

The tissue volume as well as neuronal and synaptic densities are influenced by shrinkage of the PVH, caused by fixation and other histological procedures. To be able to make corrections for shrinkage, this parameter was estimated as follows: Five male Wistar rats (200–250 g) were deeply anaesthetized with pentobarbital and placed in a stereotactic device where four small dorso-ventral holes were made at a transverse and sagittal distance of 5 mm. Subsequently, these rats were perfused and fixed overnight in the same way as described above. After removal of the brain out off the skull and fixation overnight, the distance between the four holes made was measured to estimate the shrinkage caused by perfusion and postfixation. This appeared to be $8.5 \pm 1.0\%$ linearly. After vibratomy the dimensions of the vibratome sections were measured before and after the histological procedure applied as described above. The histological procedure caused a linear shrinkage of $2.6 \pm 0.3\%$. Thus, the total linear shrinkage in our material is $10.8 \pm 1.1\%$, resulting in a three-dimensional shrinkage of $29 \pm 2.8\%$.

2.6. Statistics

Statistical analysis of differences between the two lines (APO-SUS and APO-UNSUS rats) was performed with the Mann-Whitney *U*-test. For statistical comparison of subdivisions, the Wilcoxon matched-pairs signed-ranks test was used [38].

3. Results

The results as obtained for the left PVH are summarized in Table 1, which presents values that are uncorrected for shrinkage. The effect of shrinkage will be discussed in section 4 (Table 2). A visualization of some of the light microscopic parameters determined is presented in Fig. 2. In this figure the blood vessels, neurons and subdivisions delineated in series of six representative semithin sections have been drawn separately.

3.1. Subdivisions of the PVH

In the semithin series of sections used for the present study the PVH could unequivocally be subdivided in six subdivisions on the basis of neuronal sizes and densities as well as vascular densities, as follows (see also Fig. 2):

(a) The periventricular part (PV) is a cell-sparse zone with fusiform neurons and a minor vascularization, situated along the third ventricle.

(b) The magnocellular part (MC) contains clearly larger neurons than the remaining part of the PVH. This subdivision extends laterally towards the fornix and is bordered on its lateral and ventral edges by the cell-sparse zone. The latter can easily be distinguished from the MC because of obvious difference in neuronal density and cytoarchitecture.

(c) The parvocellular part (PC), lying between the PV and MC, can be subdivided into four subdivisions on the basis of differences in vascular density, to be quantified below. The central parvocellular part (PCc) is as richly vascularized as the MC. It is bordered at the dorsal side by the dorsal parvocellular part (PCd) and ventrally by the ventral parvocellular part (PCv), both less vascularized. Posterior to the PCc, the PCd and the PCv fuse into the sparsely vascularized posterior parvocellular part (PCp).

3.2. Vascularity

The overall vascularity in the PVH, expressed as the percentage of volume occupied by blood vessels, is 5.6% (Fig. 4). The PV is the least vascularized subdivision (3.2%, $P < 0.05$). The MC is significantly more vascularized than the other subdivisions (7.8%, $P < 0.05$) except for the PCc, which has an equally rich vascular density (8.3%). The intermediate vascular densities of the PCd (4.6%), the PCv (4.6%) and the PCp (5.3%) show no significant mutual differences, but are all significantly higher than the vascular density of the PV ($P < 0.05$) and lower than the vascular densities of the MC and PCc ($P < 0.05$).

APO-SUS and APO-UNSUS rats showed no statistically significant differences in PVH vascularity except for the PV. This subdivision was slightly but significantly higher vascularized in APO-UNSUS rats (4.0%) than in APO-SUS rats (2.5%, $P < 0.05$, Table 1).

3.3. Neuronal size and shape

The mean soma diameter in the PVH is 11.8 μm, with the following differentiation between its subdivisions (Ta-

Table 1

Morphometric parameters as determined for the left PVH of 3 APO-UNSUS and 3 APO-SUS rats (mean ± S.E.M.)

Subdivisions	Vascularity (%)	Volume (mm^3)	Soma diameter (μm)	Neuronal density ($\times 10^3/mm^3$)
Overall				
PVH	5.6 ± 0.14	0.083 ± 0.0037	11.754 ± 0.177	185.4 ± 8.8
PV	3.2 ± 0.35	0.014 ± 0.0004	9.581 ± 0.182	131.8 ± 10.7
MC	7.8 ± 0.57	0.014 ± 0.0011	14.385 ± 0.264	176.7 ± 11.5
PCc	8.3 ± 0.22	0.022 ± 0.0011	10.679 ± 0.304	230.0 ± 19.4
PCd	4.6 ± 0.20	0.008 ± 0.0008	11.579 ± 0.203	185.8 ± 12.8
PCv	4.6 ± 0.28	0.009 ± 0.0007	10.979 ± 0.196	206.1 ± 16.4
PCp	5.3 ± 0.38	0.016 ± 0.0025	11.212 ± 0.197	180.6 ± 12.3
Cell-sparse zone				
APO-UNSUS				
PVH	5.8 ± 0.09	0.086 ± 0.0016	11.954 ± 0.229	172.0 ± 13.2
PV	4.0 ± 0.18	0.014 ± 0.0005	9.424 ± 0.178	137.4 ± 19.4
MC	7.1 ± 0.28	0.014 ± 0.0007	14.675 ± 0.204	157.2 ± 12.6
PCc	8.2 ± 0.35	0.022 ± 0.0016	11.068 ± 0.419	220.2 ± 35.2
PCd	4.9 ± 0.21	0.007 ± 0.0015	11.787 ± 0.351	164.1 ± 9.2
PCv	5.0 ± 0.26	0.010 ± 0.0007	11.085 ± 0.323	181.3 ± 14.7
PCp	5.7 ± 0.63	0.019 ± 0.0029	11.461 ± 0.232	170.4 ± 9.4
APO-SUS				
PVH	5.4 ± 0.37	0.076 ± 0.0059	11.575 ± 0.227	198.8 ± 5.4
PV	2.5 ± 0.33	0.013 ± 0.0005	9.737 ± 0.290	126.3 ± 13.0
MC	8.4 ± 0.97	0.013 ± 0.0021	14.096 ± 0.426	196.2 ± 11.0
PCc	8.3 ± 0.27	0.021 ± 0.0014	10.290 ± 0.304	239.8 ± 23.4
PCd	4.3 ± 0.25	0.008 ± 0.0000	11.371 ± 0.113	207.4 ± 16.1
PCv	4.2 ± 0.37	0.008 ± 0.0010	10.874 ± 0.205	230.9 ± 22.5
PCp	4.9 ± 0.28	0.012 ± 0.0029	11.010 ± 0.245	190.7 ± 23.7

Ellipticity index somata	Synaptic contact length (nm)	Synapse density ($\times 10^6/mm^3$)	S/N ratio
0.582 ± 0.004	368 ± 6	187 ± 17	1009 ± 83
0.528 ± 0.010	360 ± 12	184 ± 16	1454 ± 212
0.612 ± 0.008	385 ± 12	157 ± 22	899 ± 134
0.605 ± 0.005	364 ± 4	203 ± 21	913 ± 134
0.553 ± 0.011	400 ± 29	169 ± 33	871 ± 157
0.623 ± 0.005	341 ± 11	216 ± 18	1069 ± 115
0.569 ± 0.014	373 ± 10	185 ± 19	1025 ± 102
	351 ± 13	234 ± 13	
0.586 ± 0.008	379 ± 5	152 ± 9	893 ± 83
0.530 ± 0.009	367 ± 20	154 ± 11	1155 ± 158
0.613 ± 0.008	405 ± 11	129 ± 24	851 ± 227
0.613 ± 0.008	369 ± 3	162 ± 23	770 ± 185
0.564 ± 0.018	431 ± 48	121 ± 43	710 ± 279
0.630 ± 0.004	345 ± 20	187 ± 21	1072 ± 237
0.568 ± 0.013	393 ± 9	147 ± 17	875 ± 162
0.577 ± 0.003	357 ± 7	222 ± 15	1124 ± 120
0.525 ± 0.018	352 ± 12	214 ± 19	1753 ± 332
0.610 ± 0.013	365 ± 14	185 ± 29	946 ± 189
0.597 ± 0.001	359 ± 5	244 ± 13	1056 ± 188
0.541 ± 0.011	369 ± 21	216 ± 33	1031 ± 142
0.616 ± 0.008	337 ± 8	244 ± 19	1066 ± 100
0.571 ± 0.024	353 ± 8	223 ± 16	1175 ± 53

Table 2
Morphometric parameters of the left PVH as corrected for 10.8% linear shrinkage

Subdivisions	Volume (mm^3)	Neuornal density ($\times 10^3/mm^3$)	Synaptic density ($\times 10^6/mm^3$)
Overall			
PVH	0.117	131.6	133
PV	0.020	93.6	131
MC	0.020	125.5	111
PCc	0.031	163.3	144
PCd	0.011	131.9	120
PCv	0.013	146.3	153
PCp	0.023	128.2	131
APO-UNSUS			
PVH	0.121	122.1	108
PV	0.020	97.6	109
MC	0.020	111.6	92
PCc	0.031	156.3	115
PCd	0.010	116.5	86
PCv	0.014	128.7	133
PCp	0.027	121.0	104
APO-SUS			
PVH	0.107	141.1	158
PV	0.018	89.7	152
MC	0.018	139.3	131
PCc	0.030	170.3	173
PCd	0.011	147.3	153
PCv	0.011	163.9	173
PCp	0.017	135.4	158
Cell-sparse zone			166

ble 1): the PV contains on average the smallest neurons (9.6 μm, $P < 0.05$). These have a fusiform shape as indicated by an ellipticity index (ell.ind.) of 0.53 (Table 1). The MC contains obviously the largest neurons of the PVH (14.4 μm, $P < 0.05$), which are more rounded (ell.ind. 0.61, Table 1). The mean soma diameter of the fusiform neurons of the PCd (11.6 μm, ell.ind. 0.55, Table 1) is slightly but significantly larger that of the PCc (10.7 μm, $P < 0.05$) and the PCv (11.0 μm $P < 0.05$). The neuronal sizes observed in the PCc, PCv and PCp show no significant mutual differences. There are no statistically significant differences in neuronal size or shape between APO-SUS and APO-UNSUS rats.

3.4. Neuronal densities and numbers

The overall neuronal density in the PVH is about 185×10^3 cells/mm^3 (Fig. 4). The neuronal density of the PV ($132 \times 10^3/mm^3$) is significantly smaller ($P < 0.05$) than the neuronal density of the MC ($177 \times 10^3/mm^3$), PCc ($230 \times 10^3/mm^3$), PCd ($186 \times 10^3/mm^3$) and PCv ($206 \times 10^3/mm^3$). The neuronal density of the PCp ($181 \times 10^3/mm^3$) is, although larger, not statistically different from that of the PV. However, the difference in neuronal density between the MC and the PCc is statistically significant ($P < 0.05$). Statistical comparison between APO-UNSUS and APO-SUS rats yielded no significant differences in this respect.

The number of neurons in the PVH and its subdivisions was estimated by multiplication of the neuronal densities with the tissue volumes calculated. On average, the left PVH occupies a volume of 0.083 mm^3 and contains about 15,400 cells (Table 1). The PCc contains the largest amount of cells, about 5,000, which is 33% of the total population.

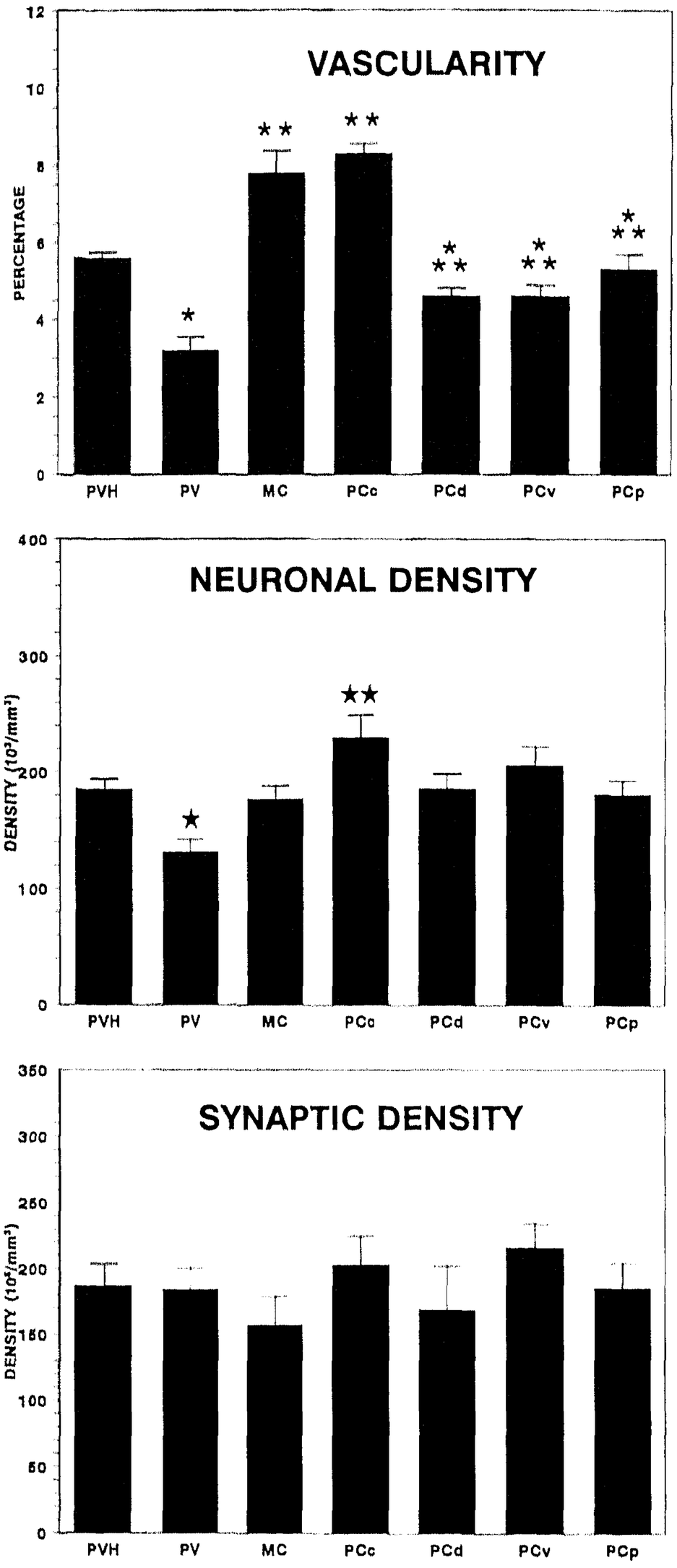

Fig. 4. Histograms of the vascular densities, neuronal densities and synaptic densities in the left PVH and its six subdivisions (mean ± S.E.M., $n = 6$). * = significantly different from MC, PCc, PCd, PCv and PCp ($P < 0.05$). ** = significantly different from PV, PCd, PCv and PCp ($P < 0.05$). *** = significantly different from PV, MC and PCc ($P < 0.05$). ★ Significantly different from MC, PCc, PCd and PCV ($P < 0.05$). ★★ Significantly different from MC ($P < 0.05$). For abbreviations see Fig. 1

The other subdivisions contribute between 12% and 19% to the total population in both APO-SUS and APO-UNSUS rats.

3.5. Synaptic contact length

The average synaptic contact trace length in the PVH is 368 nm (Table 1), which corresponds to an average synaptic contact diameter of 469 nm. The synaptic contact size is basically similar in all subdivisions as well as in the cell-sparse zone around the PVH (Table 1). The only significant difference found between subdivisions is a slightly smaller contact length in the PCv (341 nm) compared with the MC (385 nm, $P < 0.05$). Comparison of APO-SUS and APO-UNSUS rats showed that the synaptic contact length in the PCp of APO-UNSUS rats (393 nm) is significantly larger than that of APO-SUS rats (353 nm, $P < 0.05$).

3.6. Synaptic densities and numbers

The mean synaptic density in the PVH is $187 \times 10^6/mm^3$ without statistically significant differences between its subdivisions (Fig. 4). In the cell-sparse zone surrounding the PVH a similar synaptic density was observed as well. It is somewhat higher than the synaptic density in the PVH (Table 1) but this difference is not statistically significant. However, the PVH of APO-SUS and APO-UNSUS rats showed a marked difference (Fig. 5). APO-UNSUS rats have a significantly smaller overall synaptic density ($152 \times 10^6/mm^3$) than APO-SUS rats ($252 \times 10^6/mm^3$, $P < 0.05$). This difference is present in all subdivisions of the PVH (Fig. 5) and was statistically significant in our sample for the PV, PCc and PCp ($P < 0.05$). No interline difference was found in the cell-sparse zone surrounding the PVH.

Synapse numbers were estimated by multiplication of the volume of the PVH subdivisions with their synaptic density, resulting in a number of about 16×10^6 synapses in the total left PVH. The PCc contains about 29% of these synapses, the PV 17%, the MC 14%, the PCd 9%, the PCv 12% and the PCp 19%. The total number of synapses in the left PVH of APO-SUS rats (17×10^6) is considerably larger than in APO-UNSUS rats (13×10^6). However, this difference was not statistically significant in our sample, because of the large individual variations.

3.7. Synapse-to-neuron ratios

The overall synapse-to-neuron (S/N) ratio in the PVH is 1009. This means that PVH neurons have around 1000 synaptic contacts on their receptive surface, provided that they do not have dendrites outside the PVH, and that neurons outside the PVH do not have extensive dendrites within the PVH. The S/N ratio in the PV appears to be significantly higher (1454) than that in the MC (899) and PCc (913, Table 1). APO-SUS and APO-UNSUS rats are similar in this respect.

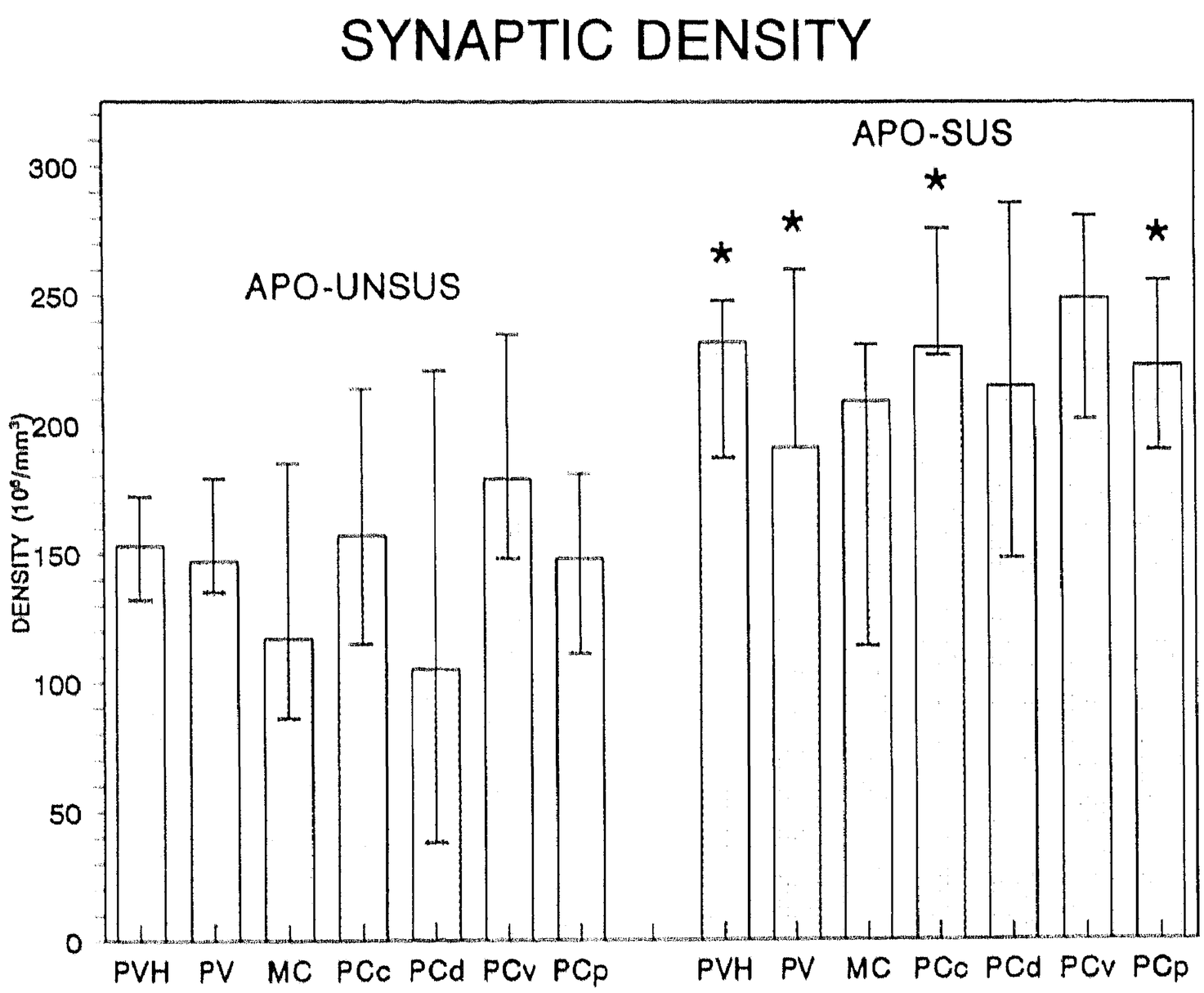

Fig. 5. Synaptic densities in APO-UNSUS ($n = 3$) and APO-SUS ($n = 3$) rats in the left PVH and its six subdivisions (median value ± highest and lowest value). * Significantly different ($P < 0.05$) from the corresponding subdivision in the APO-UNSUS rats. For abbreviations see Fig. 1.

4. Discussion

The goal of the present study is to compare the histological differentiation of the PVH of APO-SUS and APO-UNSUS rats, and to extend previous morphometric data with a quantitative characterization of the synaptic organization. In particular the latter has yielded new data showing marked differences between both rat lines. Before these differences can be evaluated in detail, a discussion on PVH subdivisions and neuronal morphometry is necessary, however, since for these aspects some striking differences with previous reports are present.

4.1. Delineation of PVH subdivisions

In the present study the PVH has been subdivided into six parts on the basis of neuronal sizes and densities as well as vascular densities. Although the latter criterion has not been used in previous studies, the resulting subdivisions correspond well to previously described ones.

All previous studies agree in the distinction of a parvocellular and a magnocellular PVH on the basis of average cell size. The laterally located magnocellular part has been further subdivided into three parts by Armstrong et al. [7]: an anterior commissural nucleus (ACN), a medial (PVM) and a lateral part (PVL). Swanson and Kuypers [42] and Swanson et al. [45] distinguished four magnocellular parts, only slightly different from the subdivisions made by Armstrong et al. [7], i.e. an anterior (AM), a medial (MP) and a posterior part (PM) that is further subdivided in a medial oxytocinergic region and a lateral vasopressinergic region. In contrast, Kiss et al. [23] considered the magnocellular section as a single entity because of the observed homogeneity in neuronal size and density. Our data are in line with the latter view (Table 1).

In the parvocellular PVH, Armstrong et al. [7] distinguished three regions: (1) the large anterior parvocellular portion (PVPA), starting immediately rostral to the PVM and projecting mainly to the median eminence, (2) the somewhat smaller dorsomedial cap (PVDC), which borders the dorsal surface of the PVH, and (3) the posterior subnucleus (PVPO), which extends dorsolaterally. In contrast to the PVPA, the latter two subdivisions contain large amounts of neurons that project to the brainstem and spinal cord [7]. Swanson and Kuypers [42] and Swanson et al. [45] distinguished six parts in the parvocellular PVH on the basis of differential projections and cytoarchitectonical characteristics: an anterior (AP), dorsal (DP), lateral (LP), periventricular (PV) and a medial (MP) part, of which the latter is further subdivided in a dorsal and medial region. Kiss et al. [23] have subdivided the parvocellular PVH on the basis of quantitative histological characteristics in a periventricular (pv) and a medial subdivision (mp), corresponding with the PV and MP of Swanson and Kuypers [42] and Swanson et al. [45] (Table 3). Within the medial subdivision they have delineated an anterior (map), a lateral (mlp), a medial (mmp) and a caudal part (mcp) on the basis of inhomogeneities in cell density. In addition, Kiss et al. [23] have distinguished a mediocellular PVH subdivision with neurons of intermediate size, subdivided into a dorsal (d) and a posterior subdivision (p), the former corresponding with the PVDC of Armstrong et al. [7] and DP of Swanson and Kuypers [42] and Swanson et al. [45], and the latter corresponding with the PVPO of Armstrong et al. [7] and LP of Swanson and Kuypers [42] and Swanson et al. [45] (Table 3).

The five parvocellular subdivisions that we distinguish in the present study, predominantly on the basis of differences in vascularity, correspond largely with the subdivisions just surveyed (Table 3). Only the PCv has never been described as a distinct subdivision, but has always been regarded as a part of another subdivision. This means that the differentiation in vascular density in the PVH offers a well defined and reproducible basis for delineations within the parvocellular PVH, resulting in similar subdivisions as distinguished previously on the basis of the histochemical, cytoarchitectonic and connectional differentiation of the PVH [7,23,42,45].

Table 3
Subdivisions of the present study and the corresponding subdivisions of previous studies

Present study	Armstrong et al. [7]	Swanson and Kuypers [42] Swanson et al. [45]	Kiss et al. [23]
PV		PV	pv
MC	PVM, PVL	PM	m
PCc	PVPA	AP, MP	map, mlp, mmp, mcp
PCd	PVDC	DP	d
PCv	PVPA	MP	p
PCp	PVPO	LP	p

Abbreviations: AP = anterior parvocellular part; d = dorsal subdivision; DP = dorsal parvocellular part; LP = lateral parvocellular part; m = magnocellular subdivision; map = medial subdivision anterior part; mcp = medial subdivision caudal part; mlp = medial subdivision lateral part; mmp = medial subdivision medial part; MP = medial parvocellular part; p = posterior subdivision; PM = posterior magnocellular part; PV/pv = periventricular part; PVDC = dorsomedial cap of the paraventricular nucleus; PVL = lateral paraventricular nucleus; PVM = medial paraventricular nucleus; PVPA = parvocellular portion of the paraventricular nucleus; PVPO = posterior portion of the paraventricular nucleus.

4.2. Vascularity of the PVH

Previous studies have shown that the blood supply to the PVH originates from the retrochiasmatic artery [5] and that the PVH is more richly vascularized than the surrounding hypothalamic region [5,47] with an overall vascular density of 3.0% [47]. In the present study we find an overall vascular density of 5.6%. This is about twice the value reported by Van den Pol [47], who excluded the periventricular part in his analysis and used only transverse sections at the level of the magnocellular subdivision. A close comparison shows that the different values reported are not caused by the mean number of vessel profiles per section surface (Van den Pol: approx. 8 per 10,000 μm^2, present study: approx. 9 per 10,000 μm^2). This means that in particular different surface areas per vessel profile are the source of the difference between both studies, in spite of the fact that both studies used similar fixation and semithin section techniques to determine vascular densities.

The vascularity of different subdivisions has never been quantified before. Only a few contradictory remarks on this subject may be found in the literature. According to Ambach and Palkovitz [5], the magnocellular part is more densely vascularized than the parvocellular part, but Van den Pol [47] claims that the magnocellular and parvocellular part are equally vascularized. Our results show that the PCc is equally vascularized as the MC, which is in accordance with Van den Pol [47]. The discrepancy with the study of Ambach and Palkovitz [5] may be caused by the fact that the parvocellular part described by Ambach and Palkovitz [5] is comparable with our combined PCc, PCd, PCv and PCp, which together indeed have a lower vascular density than the MC or the PCc separately. The low vascularity of the PV as reported in the present study, is in accordance with the observations of Van den Pol [47].

The functional relevance of the higher vascularity of the PCc and MC is uncertain. It has been suggested by Van den Pol [47] that cells in highly vascularized areas have a higher metabolic rate, correlated with the high quantities of peptides they produce and thus their higher demand for nutrients and oxygen. This would mean that the MC and PCc are the most active subdivisions of the PVH.

4.3. Neuronal properties

The present results confirm that the MC contains the largest neurons of the PVH (14.4 μm) and the PV the smallest ones (9.5 μm), while the other subdivisions consist of medium-sized neurons of about 11–12 μm. This is largely in agreement with previous studies [7,23,42,45]. Apart from a magnocellular and a parvocellular part, Kiss et al. [23] also distinguished a mediocellular region, comparable with our PCd, PCv and PCp. The cells in the PCd are indeed somewhat larger (11.6 μm, $P < 0.05$) than in the other parvocellular subdivisions. However, the cells in the PCp and PCv, also included by Kiss et al. [23] in the mediocellular subdivision, are not larger than those in other parvocellular subdivisions.

The present data on neuronal densities show in fixed tissue an overall value of 185,000 cells/mm^3, with a highest neuronal density in the PCc (230,000/mm^3) and a lowest neuronal density in the PV (132,000/mm^3, Table 1). For comparison with previous results, the present data on neuronal densities in the different subdivisions have to be corrected for shrinkage (estimated to be 10.8% linearly in our study). The results of such a correction are shown in Table 2. Compared with Kiss et al. [23], who reported a neuronal density in all regions of the PVH of around 60,000 cells/mm^3, with the exception of the pv (40,000/mm^3) and the mlp (86,000/mm^3), the presently calculated densities as corrected for shrinkage are about twice as high (PVH: 132,000/mm^3, PV: 94,000/mm^3, PCc: 163,000/mm^3, Table 2). Several factors may be involved in this discrepancy. Kiss et al. [23] quantified neuronal nuclei containing at least one nucleolus in 11 μm thick sections, whereas we quantified neuronal nuclei in semithin (1 μm) sections. However, both methods are based on the formulae of Floderus [17] and Abercrombie [2] and should yield reliable and comparable data [3,8,40], unless a substantial portion of the PVH neurons would lack a distinct nucleolus. Such neurons would be incorporated in the present study, but would not have been counted by Kiss et al. [23]. We excluded the incorporation of glial cells in our counts by comparing every drawing of a paraphenylene-diamine stained section with an adjacent toluidine blue stained section.

A factor that might be correlated with the different neuronal densities calculated is the different PVH volume reported in both studies. Kiss et al. [23] calculated an average volume of 0.18 mm^3, whereas we calculated a volume 0.12 mm^3. This might partly be the result of a different delineation of the PVH, resulting in inclusion of parts of the cell-sparse zone by Kiss et al. [23]. This would enlarge the PVH volume and reduce the overall neuronal density. However, this would also enlarge the number of neurons calculated in the PVH, which is not the case: Kiss et al. [23] reported a substantially lower number of PVH neurons than the present study. Another factor influencing the determination of the volume as well as the neuronal density of the PVH is shrinkage. The shrinkage factor used by Kiss et al. [23] (17% linearly, i.e. 43% three-dimensionally) is different from the presently used one (10.8% linearly, i.e. 29% three-dimensionally) but this relatively small difference cannot account for the large differences in calculated volumes and densities. Moreover, when the shrinkage factors applied would not represent the true values, such a deviation would not influence the neuronal numbers calculated in the PVH, which still are different in both studies. Nevertheless, delineation and shrinkage differences may still partially have their influence, since the neuronal density in the present study is two times higher,

but the neuronal number is only 1.5 times higher compared with the study of Kiss et al. [23]. Differences in rat lines used might also be involved in the different neuronal densities and PVH volumes, since Kiss et al. [23] used CFY rats, whereas we used Wistar rats. It is presently uncertain to what extent any of the factors enumerated are involved in the discrepancies just discussed.

In spite of the differences in the estimated absolute values of the neuronal densities, the mutual differences between subdivisions as presented by Kiss et al. [23] and the present study are similar. The PV has the lowest neuronal density, while the PCc, largely corresponding with the mlp of Kiss et al. [23], has the highest neuronal density. The other subdivisions have intermediate neuronal densities.

As is already mentioned above, previous estimates of the total number of cells in the PVH are considerably lower than the present results, due to the higher neuronal density observed in our study (Kiss et al. [22]: 9,000 cells, Swanson and Sawchenko [43]: 10,000 cells, Kiss et al. [23]: 10,750 cells, present study: 15,400 cells, one side). According to our results, the PV contains 12% of the total cell population, the MC 15.5%, the PCc 33% and the PCd 9.5%. This percentive distribution is largely comparable with the results of Kiss et al. [23], except for the PCv and PCp. These subdivisions together represent the posterior subdivision (p, Table 3) of Kiss et al. [23] and contain 30% of the total cell population in our study, opposite to the 16% reported by Kiss et al. [23]. In the PCc, which contains an estimated total number of 5000 cells, about 2000 CRH cells have been observed [37,44].

4.4. Synaptic characteristics

The present study is the first one giving quantitative data on the synaptic organization of the PVH. Previously reported quantitative EM data exclusively concerned the surface and number of presynaptic boutons [22]. The synaptic trace length observed in the PVH (368 ± 6 nm) is relatively large compared with other brain regions, such as the colliculus superior of rabbits [50] (241–257 nm) and rats [4] (268 nm), the visual cortex [39], (276–310 nm) and the hypothalamic aggression region [1], (267–355 nm) of rats, except for the cerebellum [21] (373 nm).

Similar to the neuronal density, the synaptic density has to be corrected for shrinkage to have an estimate of the situation in normal, unfixed, living tissue (cf. Tables 1 and 2). Our data show a similar overall synaptic density in the PVH ($133 \times 10^6/mm^3$) and the surrounding cell-sparse zone ($166 \times 10^6/mm^3$), without significant differences between PVH subdivisions. However, the synaptic density differs significantly between APO-SUS and APO-UNSUS rats, as will be discussed below. The overall synapse-to-neuron (S/N) ratio of 1009 is in agreement with the results of Kiss et al. [22] who reported the presence of about 1000 synaptic boutons per cell within the PVH.

4.5. APO-SUS versus APO-UNSUS rats

The most significant finding of the present study is the difference in synaptic density between APO-SUS ($158 \times 10^6/mm^3$) and APO-UNSUS rats ($108 \times 10^6/mm^3$) (Table 2). This is a quite specific result, since the synaptic density in the cell-sparse region surrounding the PVH is similar in both lines, as is the neuronal density in the PVH. The higher synaptic density in the PVH of APO-SUS rats compared to APO-UNSUS rats suggests the presence of a more elaborate micro-circuit in the PVH of APO-SUS rats compared to APO-UNSUS rats. This differentiation might be correlated with differences in circulating plasmacorticoid levels during early postnatal life, since it has been shown that treatment with corticosteroids retards synaptic genesis [16]. This suggests, as is hypothesized before [13,15], that APO-SUS rats are exposed to lower levels of corticosteroids than APO-UNSUS rats during early development.

It is not clear whether the higher synaptic density in the PVH of APO-SUS rats is the result of a general enhancement of synaptic development or an enhancement of one or a few specific inputs to the PVH. It is not very likely that interneurons or recurrent collaterals are involved, since these only infrequently occur in the PVH [34,47]. Previous experiments suggest a more active hypothalamo-pituitary-adrenal axis in adult APO-SUS rats compared to adult APO-UNSUS rats [15], the latter showing a significantly lower basal plasma ACTH level and a lower mineralocorticoid receptor capacity in the pituitary than the APO-SUS rats. Furthermore, it has been found that a conditioned emotional stimulus induced a higher plasma ACTH level in APO-SUS rats compared with APO-UNSUS rats [47]. Consequently, the higher synaptic density in APO-SUS rats correlates well with a presumed higher activity of the PVH during stress regulation in APO-SUS rats. However, recent work in our laboratory showed that the PVH of APO-SUS rats contains significantly less Fos-immunoreactive cells than the PVH of APO-UNSUS rats [29] after a stressful stimulus. This suggests a reduced activity of the PVH of APO-SUS rats compared to APO-UNSUS rats, which would mean that the increased synaptic density in the PVH evokes an increased inhibitory effect on the PVH. To evaluate these possibilities further, it is necessary to incorporate our Fos-experiments in detail in the discussion, which will be done in the following paper [30].

References

[1] Aalders, T.T.A. and Meek, J., The hypothalamic aggression region of the rat: observations on the synaptic organization, *Brain Res. Bull.*, 31 (1993) 229–232.

[2] Abercrombie, M., Estimation of nuclear population from microtome sections, *Anat. Rec.*, 94 (1946) 239–247.
[3] Albers, F.J., Meek, J. and Nieuwenhuys, R., Morphometric parameters of the superior colliculus of albino and pigmented rats, *J. Comp. Neurol.*, 263 (1988) 146–158.
[4] Albers, F.J., Meek, J. and Hafmans, T.G.M., Synapse morphometry and synapse-to-neuron ratios in the superior colliculus of albino rats, *J. Comp. Neurol.*, 291 (1990) 220–230.
[5] Ambach, G. and Palkovits, M., Blood supply of the rat hypothalamus. II. Nucleus paraventricularis, *Acta Morphol. Acad. Sci. Hung.*, 22 (1974) 311–320.
[6] Antoni, F.A., Palkovits, M., Makara, G.B., Linton, E.A., Lowry, P.J. and Kiss, J.Z., Immunoreactive corticotropin-releasing hormone in the hypothalamoinfundibular tract, *Neuroendocrinology*, 36 (1983) 415–423.
[7] Armstrong, W.E., Warach, S., Hatton, G.I. and McNeill, T.H., Subnuclei in the rat hypothalamic paraventricular nucleus: a cytoarchitectural, horseradish peroxidase and immunocytochemical analysis, *Neuroscience*, 5 (1980) 1931–1958.
[8] Bolender, R.P., Methods for decreasing the statistical variance of stereological estimates, *Anat. Rec.*, 207 (1983) 89–106.
[9] Born, D.E., Carman, C.S. and Rubel, E.W., Correcting errors in estimating neuron area caused by the position of the nucleolus, *J. Comp. Neurol.*, 255 (1987) 146–152.
[10] Bruhn, T.O., Plotsky, P.M. and Vale, W.W., Effect of paraventricular lesions on corticotropin-releasing factor (CRF)-like immunoreactivity in the stalk-median eminence: Studies on the adrenocorticotropin response to ether stress and exogenous CRF, *Endocrinology*, 114 (1984) 57–62.
[11] Calverley, R.K.S., Bedi, K.S. and Jones, D.G., Estimation of the numerical density of synapses in rat neocortex. Comparison of the 'dissector' with an 'unfolding' method, *J. Neurosci. Methods*, 23 (1988) 195–205.
[12] Collonier, M. and Beaulieu, C., An empirical assessment of stereological formulae applied to the counting of synaptic disks in the cerebral cortex, *J. Comp. Neurol.*, 231 (1985) 175–179.
[13] Cools, A.R., Brachten, R., Heeren, D., Willemen, A. and Ellenbroek, B., Search after neurobiological profile of individual specific features of Wistar rats, *Brain Res. Bull.*, 24 (1990) 49–69.
[14] Cools, A.R., Dierx, J., Coenders, C., Heeren, D., Ried, S., Jenks, B.G. and Ellenbroek, B., Apomorphine-susceptible and apomorphine-unsusceptible Wistar rats differ in novelty-induced changes in hippocampal dynorphin B expression and two-way active avoidance: a new key in the search for the role of the hippocampal-accumbens axis, *Behav. Brain Res.*, 55 (1993) 213–221.
[15] Cools, A.R., Rots, N.Y., Ellenbroek, B. and de Kloet, E.R., Bimodal shape of individual variation in behavior of Wistar rats: the overall outcome of a fundamentally different make-up and reactivity of the brain, the endocrinological and the immunological system, *Neuropsychobiology*, 28 (1993) 100–105.
[16] De Kloet, E.R., Rosenfeld, P., Van Eekelen, J.A.M., Sutanto, W. and Levine, S., Stress, glucocorticoids and development. In G.J. Boer, M.G.P. Feenstra, M. Mirmiran, D.F. Swaab and F. Van Haaren (Eds.), *Prog. Brain Res.*, 1988, pp. 101–120.
[17] Floderus, S., Untersuchungen über den bau der menschlichen hypophyse mit besonderer berücksichtigung der qualitativen mikromorphologischen verhältnisse, *Acta Pathol. Microbiol. Scand.*, 5 (1944) 1–26.
[18] Gundersen, H.J.G., Notes on the estimation of the numerical density of arbitrary profiles: the edge effect, *J. Microsc.*, 111 (1977) 219–223.
[19] Gundersen, H.J.G. and Jensen, E.B., The efficiency of systematic sampling in stereology and its prediction, *J. Microsc.*, 147 (1987) 229–263.
[20] Haas, D.A. and George, S.R., Single or repeated mild stress increases synthesis and release of hypothalamic corticotropin-releasing factor, *Brain Res.*, 461 (1988) 230–237.
[21] Hillman, D.E. and Chen, S., Compensation in the number of presynaptic dense projections and synaptic vesicles in remaining parallel fibres following cerebellar lesions, *J. Neurocytol.*, 14 (1985) 673–687.
[22] Kiss, J.Z., Palkovits, M., Zaborszky, L., Tribollet, E., Szabo, D. and Makara, G.B., Quantitative histological studies on the hypothalamic paraventricular nucleus in rats. I. Number of cells and synaptic boutons, *Brain Res.*, 262 (1983) 217–224.
[23] Kiss, J.Z., Martos, J. and Palkovits, M., Hypothalamic paraventricular nucleus: A quantitative analysis of cytoarchitectonic subdivisions in the rat, *J. Comp. Neurol.*, 313 (1991) 563–573.
[24] Lechan, R.M., Nestler, J.L., Jacobson, S. and Reichlin, S., The hypothalamic 'tuberoinfundibular' system of the rat as demonstrated by horseradish peroxidase (HRP) microiontophoresis, *Brain Res.*, 195 (1980) 13–27.
[25] Mayhew, T.M., Stereological approach to the study of synapse morphometry with particular regard to estimating number in a volume and on a surface, *J. Neurocytol.*, 8 (1979) 121–138.
[26] Mayhew, T.M. and Olsen, D.R., Magnetic resonance imaging (MRI) and model-free estimates of brain volume determined using the Cavalieri principle, *J. Anat.*, 178 (1991) 133–144.
[27] Michel, R.P. and Cruz-Orive, L.M., Application of the Cavalieri principle and vertical sections method to lung: estimation of volume and pleural surface area, *J. Microsc.*, 150 (1988) 117–136.
[28] Moldow, R.L., Kastin, A.J., Graf, M. and Fischman, A.J., Stress mediated changes in hypothalamic corticotropin releasing factor-like immunoreactivity, *Life Sci.*, 40 (1987) 413–418.
[29] Mulders, W.H.A.M., Meek, J., Hafmans, T.G.M., Veening, J.G. and Cools, A.R., c-*fos* activity in the hypothalamic paraventricular nucleus after open-field stress: comparison of two different pharmacogenetically selected strains of rats, *Eur. J. Neurosci.*, Suppl., 6 (1993) 781.
[30] Mulders, W.H.A.M., Meek, J., Schmidt, E.D., Hafmans, T.G.M. and Cools, A.R., The hypothalamic paraventricular nucleus in two types of Wistar rats with different stress responses. II. Differential Fos-expression, *Brain Res.*, 689 (1995) 61–70.
[31] Peduzzi, J.D. and Crossland, W.J., Anterograde transneuronal degeneration in the ectomammilary nucleus and ventral lateral geniculate nucleus of the chick, *J. Comp. Neurol.*, 213 (1983) 287–300.
[32] Plotsky, P.M., Regulation of hypophysiotropic factors mediating ACTH secretion, *Ann. NY Acad. Sci. USA*, 512 (1987) 205–217.
[33] Regeur, L. and Pakkenberg, B., Optimizing sampling designs for volume measurements of components of human brain using a stereological method, *J. Microsc.*, 155 (1989) 113–121.
[34] Rho, J.-H. and Swanson, L.W., A morphometric analysis of functionally defined subpopulations of neurons in the paraventricular nucleus of the rat with observations on the effects of colchicine, *J. Neurosci.*, 9 (1989) 1375–1388.
[35] Rivier, C., Rivier, J. and Vale, W., Inhibition of adrenocorticotropic hormone secretion in the rat by immunoneutralization of corticotropin-releasing factor, *Science*, 218 (1982) 377–379.
[36] Royet, J.-P., Stereology: a method for analyzing images, *Prog. Neurobiol.*, 37 (1991) 433–474.
[37] Sawchenko, P.E. and Swanson, L.W., Localization, colocalization and plasticity of corticotropin-releasing factor immunoreactivity in rat brain, *Fed. Proc.*, 44 (1985) 221–227.
[38] Siegel, S., *Non-Parametric Statistics for the Behavioral Sciences*, McGraw-Hill, New York, 1956, pp. 75–83, 116–127.
[39] Sirevaagh, A.M. and Greenough, W.T., Differential rearing effects on rat visual cortex synapses. II. Synaptic morphometry, *Dev. Brain Res.*, 19 (1985) 215–226.
[40] Smolen, A.J., Wright, L.L. and Cunningham, T.J., Neuron numbers in the superior cervical sympathetic ganglion of the rat: a critical comparison of methods for cell counting, *J. Neurocytol.*, 12 (1983) 739–750.
[41] Sutanto, W., de Kloet, E.R., de Bree, F. and Cools, A.R., Differential corticosteroid binding characteristics to the mineralocorticoid

(type I) and glucocorticoid (type II) receptors in the brain of pharmacogenetically-selected apomorphine-susceptible and apomorphine-unsusceptible wistar rats, *Neurosci. Res. Commun.*, 5 (1989) 19–26.

[42] Swanson, L.W. and Kuypers, H.G.J.M., The paraventricular nucleus of the hypothalamus: cytoarchitectonic subdivisions and organization of projections to the pituitary, dorsal vagal complex, and spinal cord as demonstrated by retrograde fluorescence double-labeling methods, *J. Comp. Neurol.*, 194 (1980) 555–570.

[43] Swanson, L.W. and Sawchenko, P.E., Hypothalamic integration: organization of the paraventricular and supraoptic nuclei, *Ann. Rev. Neurosci.*, 6 (1983) 269–324.

[44] Swanson, L.W., Sawchenko, P.E., Rivier, J. and Vale, W.W., Organization of ovine corticotropin-releasing factor immunoreactive cells and fibers in the rat brain: an immunohistochemical study, *Neuroendocrinology*, 36 (1983) 165–186.

[45] Swanson, L.W., Sawchenko, P.E. and Lind, R.W., Regulation of multiple peptides in CRF parvocellular neurosecretory neurons: Implications for the stress response. In T. Hökfelt, K. Fuxe and B. Pernaw (Eds.), *Progr. Brain Res.*, Elsevier, Amsterdam, 68, 1986, pp. 169–190.

[46] Vale, W., Spiess, J., Rivier, C. and Rivier, J., Characterization of a 41-residue ovine hypothalamic peptide that stimulates secretion of corticotropin and β-endorphin, *Science*, 213 (1981) 1394–1397.

[47] Van den Pol, A.N., The magnocellular and parvocellular paraventricular nucleus of rat: intrinsic organization, *J. Comp. Neurol.*, 206 (1982) 317–345.

[48] Van Eekelen, J.A.M., Rots, N.Y., de Kloet, E.R. and Cools, A.R., Central corticoid receptors and stress responsiveness in two pharmacogenetically selected rat lines, *Soc. Neurosci. Abstr.*, 18 (1992) 1514.

[49] Van Oers, J.W.A.M., Hinson, J.P., Binnekade, R. and Tilders, F.J.H., Physiological role of corticotropin-releasing factor in the control of adrenocorticotropin-mediated corticosterone release from the rat adrenal gland, *Endocrinology*, 130 (1992) 282–288.

[50] Vrensen, G. and De Groot, D., Quantitative aspects of the synaptic organization of the superior colliculus in control and dark-reared rabbits, *Brain Res.*, 134 (1977) 417–428.

[51] Weibel, E.R., Practical methods for biological morphometry, In E.R. Weibel (Ed.),*Stereological methods. Vol. 1*, Academic press., NY, 1979, 9–62, 101–160.

[52] Whitnall, M.H., Smyth, D. and Gainer, H., Vasopressin coexists in half of the corticotropin-releasing factor axons present in the external zone of the median eminence in normal rats, *Neuroendocrinology*, 45 (1987) 420–424.